

# Modeling and analysis of field-oriented control based permanent magnet synchronous motor drive system using fuzzy logic controller with speed response improvement

Parvathy Thampi Mooloor Sahridayan<sup>1</sup>, Raghavendra Gopal<sup>2</sup>

<sup>1</sup>Department of Electrical and Electronics Engineering, CMR Institute of Technology, Bengaluru, India

<sup>2</sup>Department of Electrical and Electronics Engineering, Sapthagiri College of Engineering, Bengaluru, India

## Article Info

### Article history:

Received Jun 23, 2021

Revised Jun 20, 2022

Accepted Jul 10, 2022

### Keywords:

Field-oriented control  
Fuzzy logic controller  
Permanent magnet synchronous motor  
Proportional-integral-derivative controller  
Speed response  
Torque

## ABSTRACT

The permanent magnet synchronous motor (PMSM) acts as an electrical motor mainly used in many diverse applications. The controlling of the PMSM drive is necessary due to frequent usage in various systems. The conventional proportional-integral-derivative (PID) controller's drawbacks are overcome with fuzzy logic controller (FLC) and adopted in the PMSM drive system. In this manuscript, an efficient field-oriented control (FOC) based PMSM drive system using a fuzzy logic controller (FLC) is modeled to improve the speed and torque response of the PMSM. The PMSM drive system is modeled using abc to  $\alpha\beta$  and  $\alpha\beta$  to abc transformation, 2-level space vector pulse width modulation (SVPWM), AC to DC rectifier with an inverter, followed by PMSM drive, proportional integral (PI) controller along with FLC. The FLC's improved fuzzy rule set is adopted to provide faster speed response, less % overshoot time, and minimal steady-state error of the PMSM drive system. The simulation results of speed response, torque response, speed error, and phase currents are analyzed. The FLC-based PMSM drive is compared with the conventional PID-based PMSM drive system with better improvements in performance metrics.

This is an open access article under the [CC BY-SA](https://creativecommons.org/licenses/by-sa/4.0/) license.



## Corresponding Author:

Parvathy Thampi Mooloor Sahridayan  
Department of Electrical and Electronics Engineering, CMR Institute of Technology  
Bengaluru, Karnataka, India  
Email: parvathy.t@cmrit.ac.in

## 1. INTRODUCTION

The control system-based permanent magnet synchronous motor (PMSM) drives are used extensively in AC speed drives systems with diverse fields like power electronics, sensors, high-speed microprocessors, automatic control systems, magnetic materials, and special-featured converters. The PMSM drive system has many advantages: rapid dynamic response, low noise, high power factor, efficiency, and high torque-inertia ratio. The PMSM drive is extensively used in many domestic and industrial drive applications due to the motor's high-speed range operations, high power density, and high efficiency. The robustness and reliability are increased due to the use of drives without machine-mounted sensors. These mounted sensors offer low-cost operations in a system with more reliability [1], [2]. The high-performance PMSM drive system provides a more significant dynamic response, strong robustness, better speed regulation, and higher reliability over direct current (DC) and brushless DC (BLDC) motors.

The permanent magnets are distributed into surface and interior (SPMSM and IPMSM) based on PMSM classification. Similarly, based on field flux, the PMSM is classified into radial and axial fields. Finally, the mechanical sensors are installed in real-time on the rotor shaft to get accurate speed response and

rotor position information using a conventional approach. But these approaches may lead to issues like a decrease in robustness and reliability and an increase in volume, cost, and inertia. So PMSM based sensor-less control strategies are used to improve the cost and performance. The sensor-less control mechanism is used to perform the control and sensing operation by the machine itself without using any mechanical sensors. The sensor-less control mechanism is classified based on the speed of the motor like initial position detection (IPD) technique, low-speed, mid-speed, and high-speed control techniques. The IPD technique has to rotate and pulsating high-frequency injection techniques, test signal injection techniques, and inductance matrix methods. The low-speed control techniques have voltage/frequency (V/F) and I/F control methods. Finally, the mid-speed control techniques contain the back-electromotive force (EMF) technique, extended Kalman filter, reference adaptive system sliding-mode observer, and artificial neural network (ANN) based techniques. At last, the full-speed control approach contains a combination of low-speed and mid-speed control techniques [1]–[5]. The PMSM drive system produces torque ripples, which affect the overall dynamic response of the motors. The repetitive current control [6] and digital observer controller [7] approaches are available to minimize the torque ripples. The speed control mechanism is improved using fuzzy logic controller, adaptive fuzzy logic controller (FLC), and FLC-PI-based methods in the PMSM drive systems [8]–[10].

In this manuscript, an efficient field-oriented control (FOC-based) PMSM drive system using FLC is modeled. The contribution of the research work is highlighted: i) the space vector pulse width modulation (SVPWM) is introduced in the FOC-based PMSM drive system to provide better gate pulses for an inverter with proper DC utilization; ii) the proposed model can work for any significant torque load with different configurations and achieves moderate dynamic responses; iii) the fuzzy rules are improvised with proper display range, providing a better speed response, less steady-state error, less overshoot time, and better anti-interference ability in the PMSM drive system; and iv) the proposed work offers better speed and torque response than the proportional-integral-derivative (PID) controller based PMSM.

The manuscript is organized: the existing approaches of PMSM using conventional PID and fuzzy logic controllers are discussed in below section. The modeling of the PMSM drive is discussed with mathematical equations in section 2. The controlling proposed strategies for PMSM are discussed in section 3. Section 4 discusses the simulation and performance results of the FLC-based PMSM drive system compared with the conventional PI-based PMSM drive system. Finally, it concludes the overall work with futuristic scope in section 5.

This section discusses the related work of the PMSM drive system using different control strategies and analyzes the performance metrics. First, Na and Wang [11] present the improved vector control mechanism for PMSM based FLC. The speed and current controllers are designed using modified controlling strategies like integral separation and fuzzy-PI double mode methods. Compared with the conventional proportional integral (PI) controller, the recent work improves dynamic responses and other performance metrics. Next, Iqbal *et al.* [12] discuss the surface mount PMSM drive using adaptive FLC. The work replaces the conventional PI speed controller with adaptive FLC to control the motor drive's control response. The model analyzes the PMSM speed response with and without load conditions for PI and adaptive FLC controllers. The work is illustrated on the DSP hardware module and analyzes the performance parameters.

Singh *et al.* [13] discuss the performance comparison of PI and FLC-based controllers for PMSM drive systems. The FLC-based PMSM drives analyze the simulation results for no-load, full load, and varying load using torque. The work concludes that the FLC-based PMSM drives give better performance than the PI-based PMSM drive. Finally, Umabharathi and Vijayabaskar [14] present the evolutionary fuzzy PID controller based PMSM system for speed control. The evolutionary algorithm (EA) offers guaranteed closed-loop stability and a better speed control mechanism. The EA is used to auto-tune the fuzzy-based PID controller's control parameter values and is suitable for real-time scenarios.

Lazarescu *et al.* [15] discuss the speed control technique using FLC for the PMSM drive. The work uses FLC with reduced perturbations to improve the dynamic response of the PMSM. The FLC is designed using two rules: 25 and the other is 49, which analyzes the speed and torque response with time variations. Liu *et al.* [16] discuss the stability analysis approach for PMSM using adaptive fuzzy PID controller. The equivalent s-domain model and PID controller with adaptive fuzzy PID controllers are used for stability analysis. Samat *et al.* [17] discuss the PMSM based Takagi-Sugeno (T-S) FLC for speed control analysis. The results are analyzed for FLC-based PMSM under no-load, full load, and variable load conditions. The speed and torque response, speed error dq-current response is represented with simulation results. Rathod *et al.* [18] present the PMSM drive system using an Adaptive control mechanism for Electric vehicles. The Adaptive control mechanism is incorporated as an observer, which estimates the actual torque feedback value with linearization.

Gaeid *et al.* [19] discuss the PMSM motor simulation with 5-phase inverter control using transformation methods. The Mathematical model of PMSM is designed as a mechanical part, and the vector transformation methods are modeled as the electrical part of PMSM. The signal processing techniques like

discrete wavelet transformation (DWT) and short-time Fourier transform (STFT) methods control the fault in the PMSM system. Lu *et al.* [20] present the adaptive control strategy of PMSM using a fuzzy PID controller. The three fuzzy control logic uses three different gain factors (PID) to improve speed and reduce speed errors. Hu and Zhang [21] explain the PMSM vector control mechanism using a fuzzy PI controller. The work discusses the FLC in detail with the working principle. It analyzes the simulation results of speed response, torque response, contrast overshoot, speed comparison of PI and FLC under sudden load changes. Kakouche *et al.* [22] present the PMSM model with minimum flux and torque ripples using the FLC approach. The direct torque control approach replaces the conventional hysteresis controllers with two FLC to reduce the current, flux, and torque ripples.

Xue *et al.* [23] present the PMSM model with a position tracking method modeled for robot systems. The work uses an improved version of the fuzzy back-stepping approach with position tracking for manipulator drive. The improved version of fuzzy membership rules supports solves fundamental fuzzy logic issues like a steady-state error. Using the fuzzy back-stepping control method, the work analyzes fuzzy member function with different approaches like position tracking, trajectory error, and position trajectory. Balashanmugham and Maheswaran [24] discuss the PMSM drives, including PMSM types, modeling, and control techniques. The FOC based PMSM model incorporates the FLC with SVPWM to improve the performance and dynamic response. The FLC with SVPWM for PMSM provides better torque ripple factors than the existing control strategies. Urbanski and Janiszewski [25] discuss the sensorless control strategies of the PMSM drive. The work includes two estimator approaches for PMSM drive using unscented Kalman filter, observer, and reference model. The work offers more accurate speed control and dq-axis stator currents by concerning the reference values. Hadi and Ibraheem [26] present the surface mount PMSM using a genetic algorithm with a tracking differentiator (TD) PID control approach. The TD provides the necessary transient values for given reference speed and obtained speed values.

## 2. OVERVIEW OF FOC BASED PMSM

The FOC is one of the vector control mechanisms in the AC motor control system. The FOC controls the torque and flux independently using vector transformation techniques and space vector theory. In addition, the FOC controls the dq current/voltages and manages the three-phase voltage/currents. The FOC mainly controls any synchronous motor that changes the load conditions in a wide range of speed applications with adjustable speed features.

### 2.1. Vector transformation

The representation of three-phase current ( $I_{abc}$ ) in FoC into a complex vector  $I_s$  and converting into a 2-level orthogonal stationary reference frame (SRF). The conversion process is known as Clark transformation, which has two stationary quadrature current values ( $I_\alpha$  and  $I_\beta$ ). The Park transformation process converts the orthogonal SRF into a 2-level orthogonal rotating reference frame (RRF) using rotor flux positioning. This Park transformation is used to terminate the time-varying inductance values from the AC machine's voltage equations. The park transformed values ( $I_q$  and  $I_d$ ) remain constant under steady-state conditions and are controlled by two PI controllers. The  $I_q$  and  $I_d$  are q-axis and d-axis stator current and related to torque and flux. The three-phase current to two-level RRF are represented using (1) and (2):

$$I_q = \frac{2}{3} [I_a \cos\theta + I_b \cos(\theta - 2\pi/3) + I_c \cos(\theta + 2\pi/3)] \quad (1)$$

$$I_d = -\frac{2}{3} [I_a \sin\theta + I_b \sin(\theta - 2\pi/3) + I_c \sin(\theta + 2\pi/3)] \quad (2)$$

The direct proportion between d-axis current and torque are occurred by fixing the reference d-axis current to zero ( $I_{dref}=0$ ). The remaining reference q-axis current ( $I_{qref}$ ) has happened with the help of a FLC. The 2-level RRF returns to SRF using inverse Park transformation and has two reference voltage vector variables ( $V_\alpha$  and  $V_\beta$ ). These voltage variables are converting back to three-phase SRF using inverse Clark transformation. The Three-phase Voltage is represented using (3):

$$\begin{aligned} V_a &= V_q \cos\theta + V_d \sin\theta \\ V_b &= V_q \cos(\theta - 2\pi/3) - V_d \sin(\theta - 2\pi/3) \\ V_c &= V_q \cos(\theta + 2\pi/3) - V_d \sin(\theta + 2\pi/3) \end{aligned} \quad (3)$$

The three-phase reference voltage variables ( $V_{abc}$ ) are converted to two-level SRF ( $V_\alpha$  and  $V_\beta$ ) using Clark transformation, and these are input to 2-level SVPWM process.

## 2.2. Modelling of PMSM

The mathematical model of FOC-based PMSM is set with a fixed reference frame to understand the vector control principles. The PMSM dynamic model is determined using 2-phase motor direct (d) and quadrature (q) axes. The dq-model of the PMSM drive is derived from the synchronous machine without damping winding and field current dynamics. The PMSM dynamic model is derived with few assumptions. Considering the balanced three-phase supply voltage, Stator winding has an equal number of turns. The induced EMF has sinusoidal features, Hysteresis losses, eddy currents, and saturation are not considered.

The rotating transformation concept provides more significant simplification in the electrical equation derivations. The interior PMSM has two-axis stator voltage (4) and (5) for stator winding:

$$V_q = R_s I_q + W_r \lambda_d + \rho \lambda_q \quad (4)$$

$$V_d = R_s I_d - W_r \lambda_q + \rho \lambda_d \quad (5)$$

The flux linkage is defined for q-axis  $\lambda_q = L_q I_q$  and for d-axis  $\lambda_d = L_d I_d + \lambda_f$ . Substitute the  $\lambda_q$  and  $\lambda_d$  values to (4) and (5). So, the voltage equations in the matrix form are represented in (6):

$$\begin{pmatrix} V_q \\ V_d \end{pmatrix} = \begin{pmatrix} R_s + \rho L_q & W_r L_d \\ -W_r L_q & R_s + \rho L_d \end{pmatrix} \begin{pmatrix} I_q \\ I_d \end{pmatrix} + \begin{pmatrix} \lambda_f W_r \\ \lambda_f \rho \end{pmatrix} \quad (6)$$

$V_d$  and  $V_q$  are dq-axis stator voltages,  $I_d$  and  $I_q$  are dq -axis stator currents. The  $\lambda_f$  is flux linkage due to the rotor magnets linking the stator;  $\lambda_d$  and  $\lambda_q$  are the dq-axis stator flux linkages.  $\rho$  is the derivative operator,  $R_s$  stator winding resistance,  $L_d$  and  $L_q$  are dq-axis inductances.  $W_r$  is electrical speed, and  $\theta$  is rotor position.

The electromagnetic torque (EMT) is a PMSM output variable used to calculate the machines mechanical dynamics (rotor speed and position). The generated EMT is represented in (7).

$$T_{em} = \frac{3}{2} P \lambda_f I_q + \frac{3}{2} P (L_d - L_q) I_d I_q \quad (7)$$

The 1<sup>st</sup> term from (7) is mutual reaction torque between  $I_q$  and Magnet. Whereas the 2<sup>nd</sup> term is reluctance torque, which is obtained using the d-axis and q-axis Inductance difference. The mechanical EMT is represented in (8):

$$T_{em} = T_L + W_m B + J \frac{dW_m}{dt} \quad (8)$$

$T_L$  is torque load,  $W_m$  is the rotor's angular velocity (mechanical),  $B$  is viscous friction coefficient,  $P$  is a number of pole pairs.

## 3. CONTROLLING MECHANISM FOR PMSM DRIVE

The FOC-based PMSM system process is started only when the synchronous motor produces the three-phase current ( $I_{abc}$ ) and rotor angle ( $\theta$ ). This three-phase stator current ( $I_{abc}$ ) is input to the Clark transformation, with the 2-level current vectors ( $I_\alpha$  and  $I_\beta$ ). The Park transformation is used to convert the 2-level current vectors ( $I_\alpha$  and  $I_\beta$ ) into 2-level torque ( $I_q$ ) and flux current ( $I_d$ ). The values of  $I_q$  and  $I_d$  depend upon the rotor flux position and two current vector values. The flux current ( $I_d$ ) and torque current ( $I_q$ ) are controlled independently with the help of FOC-based PMSM. Hence the  $I_q$  and  $I_d$  values are compared with reference torque and flux currents ( $I_{qref}$  and  $I_{dref}$ ). The reference torque current ( $I_{qref}$ ) is calculated using a fuzzy logic controller, and the reference Flux current ( $I_{dref}$ ) is set to zero under steady-state conditions. At the same time, these stator currents ( $I_d$ , and  $I_q$ ) are used to control the PMSM drive system by tuning the reference torque and flux currents ( $I_{qref}$  and  $I_{dref}$ ). The FOC-based PMSM driven system using FLC and SVPWM is represented in Figure 1.

The FLC acts as a speed controller, which initially starts with a reference speed of 400 rad/s. The FLC has two inputs and one output variable. The FLC receives speed error has a first input, and the change in speed error has a second input. The FLC is set with a membership function that uses 49 rule sets through the fuzzy and defuzzification process. The FLC output acts as a reference torque current ( $I_{qref}$ ) and input to one PI controller. The PI controllers act as current controllers, receive reference torque and flux current ( $I_{qref}$  and  $I_{dref}$ ), and generate the two-reference voltage variables ( $V_q$  and  $V_d$ ). Using inverse park transformation, these  $V_q$  and  $V_d$  voltage variables are converted to two voltage vectors ( $V_\alpha$  and  $V_\beta$ ). The values of  $V_\alpha$  and  $V_\beta$  are processed further to generate a three-phase voltage ( $V_{abc}$ ) using inverse Clark transformation.

In the proposed work, the 2-level SVPWM is used to drive the proper gate pulses to the inverter to smoothen the dynamic response and improve the performance parameters of the motor drive. Hence, the three-phase voltage ( $V_{abc}$ ) is converted back to 2-level voltage vectors ( $V_\alpha$  and  $V_\beta$ ) using Clark transformation and is input to the 2-level SVPWM. Next, the SVPWM is used to calculate the switching patterns of the upper three transistors of the inverter. The eight possible phase voltage configurations are obtained using eight different combinations of the ‘on’ and ‘off’ states of the upper three transistors. The rotary magnetic field (circular based) is obtained using the pulse width modulation (PWM) method, which controls the PMSM drive based on the switching activity of the space voltage vectors. The SVPWM produces the six gate pulses and is input to the inverter process. The inverter receives the DC voltage using AC to DC rectifier and produces the three-phase voltage/current for the PMSM drive. Lastly, the PMSM drive delivers the rotor angle ( $\theta$ ), stator currents (dq-axis), rotor speed ( $W_m$ ), and electromagnetic torque ( $T_{em}$ ) parameters. These parameters are used to analyze the dynamic response and performance metrics of the PMSM drive.

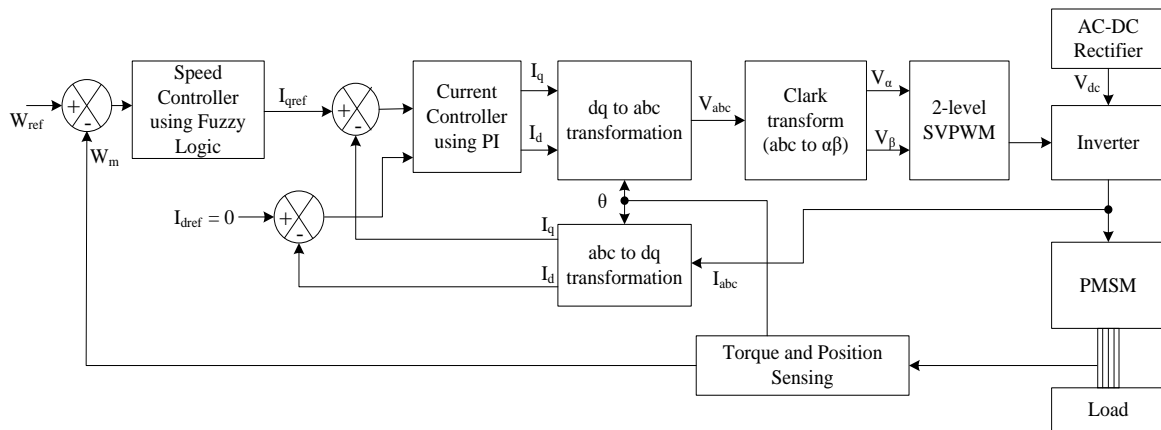


Figure 1. FOC based PMSM driven system using FLC and SVPWM

### 3.1. Fuzzy logic controller

The utilization of human experience and knowledge for the controller design application process is the fuzzy logic controller’s motivation. The FLC collects fuzzy variables to use directly into the application process instead of the complex dynamic model. The high-performance speed control mechanism is achieved using FLC with the PI controller in a closed-loop control system. The FLC enhances the dynamic response and other performance metrics by limiting the reference current for torque development [27], [28]. The general block diagram of the FLC with process is represented in Figure 2. It mainly contains four blocks: fuzzification, rule or knowledge base, inference engine, and defuzzification. The fuzzification transforms the crisp (real) variables into fuzzy (linguistic) variables. The rule or knowledge base collects the fuzzy variables and control rules knowledge from the human decision process to achieve the decision-making logic or objective. The inference engine is also known as fuzzy inference or mechanism, which is used to conclude the control action mechanism for the given fuzzy inputs by performing different fuzzy logic operations. The defuzzification process transforms the inferred fuzzy control action into the required crisp (real) variables. These crisp variables are used further into the system process (PMSM drive).

#### 3.1.1. Input and output variables

The FLC uses speed error ( $e$ ) and change in speed error ( $\Delta e$ ) as fuzzy input variables and produces the  $I_{qref}$  as fuzzy output variable. The speed error ( $e$ ) and change in speed error ( $\Delta e$ ) is defined in (9) and (10):

$$e(i) = W_{ref} - W_m \quad (9)$$

$$\Delta e(i) = e(i) - e(i - 1) \quad (10)$$

The difference between reference speed ( $W_{ref}$ ) and actual rotor speed ( $W_m$ ) values determines the speed error ( $e$ ) value. The fuzzy logic with PI controllers for PMSM is represented in Figure 3.

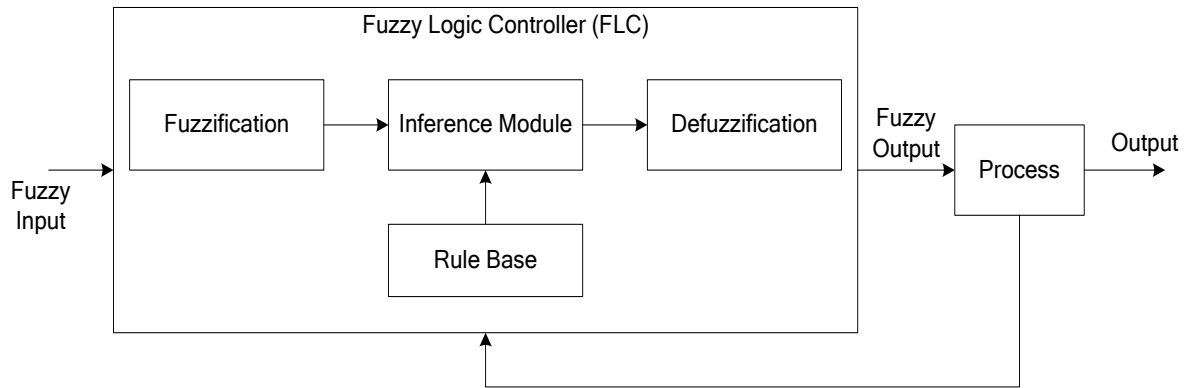


Figure 2. General block diagram of FLC with process

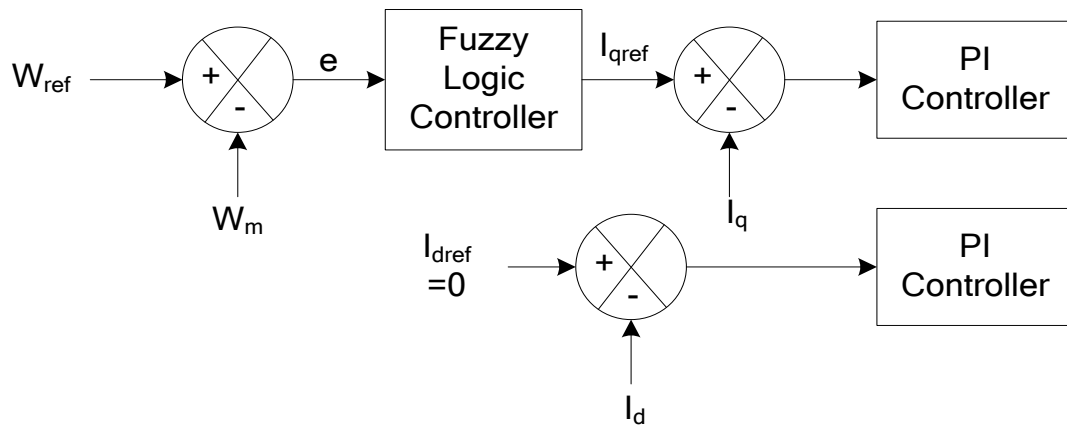


Figure 3. Representation of FLC with PI controllers for PMSM

**3.1.2. Membership function**

Both the inputs ( $e$  (i) and  $\Delta e$  (i)) is normalized to the display range -400 to 400 using a set of membership functions for the given universe of discourse. In contrast, fuzzy output is also set with -400 to 400 under the given universe of discourse. Input fuzzy variables control the degree of membership with various classes. Each fuzzy input variable has seven fuzzy values in this FLC design and is considered under the triangular membership function type.

The two fuzzy inputs and one FLC output contains seven fuzzy values individually and are negative-large (NL), medium (NM), small (NS), zero (ZE), positive-large (PL), medium (PM), and small (PS). The development of FLC for speed control in PMSM is represented in Figure 4. The membership function plots for the fuzzy inputs like speed error ( $e$ ) and change in speed error ( $\Delta e$ ) are represented in Figures 4(a) and 4(b), respectively. The membership function plot for the FLC output and FLC surface view is illustrated in Figures 4(c) and 4(d).

**3.1.3. Fuzzy rules**

The two crisp inputs are converted to fuzzy variables and later mapped into linguistic labels in the fuzzification process. The fuzzy interface system (FIS) provides the rule base, expressed as IF-THEN rules as tabulated in Table 1. The membership functions are associated with each linguistic label, which contains two fuzzy inputs and one output. The two inputs are connected in AND fashion in FIS. The Mamdani FIS is used in the current FLC design process. This rule base contains 49 rules, which transforms the two fuzzy input variables into a single output. In addition, it provides motor speed information to be the desired speed values by altering PI parameters. In the end, the fuzzy results in the rule base are converted to crisp and executable output using defuzzification with the centroid process.

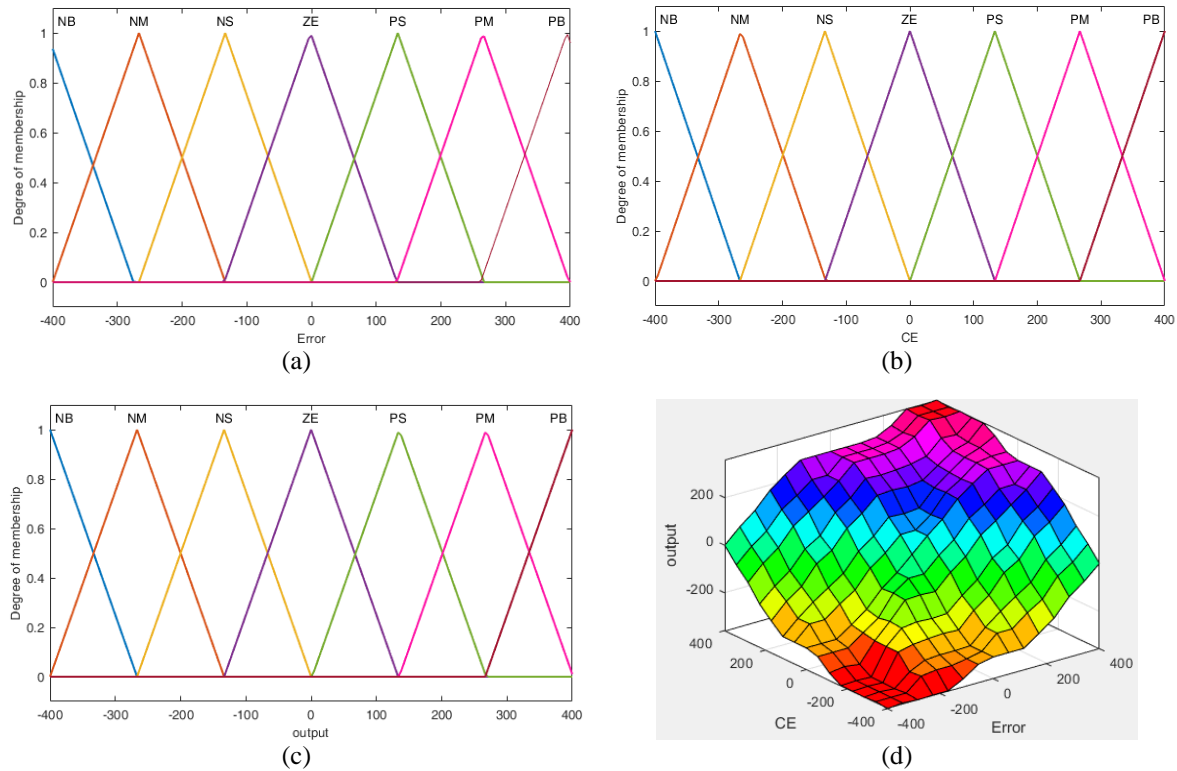


Figure 4. Development of FLC for speed control in PMSM, (a) FLC error input, (b) FLC change in error input, (c) FLC output, and (d) surface view of FLC

Table 1. Rule base for FLC

Error/CE	NB	NM	NS	ZE	PS	PM	PB
NB	NB	NB	NB	NM	NM	NS	ZE
NM	NB	NB	NB	NM	NS	ZE	PS
NS	NB	NM	NS	NS	ZE	PS	PM
ZE	NM	NM	NS	ZE	PS	PM	PM
PS	NM	NS	ZE	PS	PS	PM	PB
PM	NS	ZE	PS	PM	PM	PB	PB
PB	ZE	PS	PM	PM	PB	PB	PB

**4. RESULTS AND DISCUSSION**

The PMSM drive is modeled using PID/FLC controller with a 2-level SVPWM. The simulation is carried out under the MATLAB/Simulink environment. Speed response, speed error, torque, current parameters are analyzed with simulation results of PMSM drive. The PID controller and FLC are considered a speed controller and simulated individually to analyze the performance metrics. The dynamic response and characteristics of the PMSM are analyzed under different torque load scenarios. The reference speed of the PMSM is fixed to 400 rpm and explore in different torque load scenarios. The PMSM drive parameter specification is tabulated in Table 2. The Simulink modeling of PMSM drive using PID or FLC with 2-level SVPWM is represented in Figure 5.

Table 2. PMSM specifications

Parameters	Values
PMSM Drive	
Stator resistance (Rs)	Stator resistance (Rs)
D-axis inductance (Ld)	D-axis inductance (Ld)
Q-axis inductance (Lq)	Q-axis inductance (Lq)
Flux linkage ( $\lambda_f$ )	Flux linkage ( $\lambda_f$ )
Inertia (J)	Inertia (J)
Friction factor (B)	Friction factor (B)
Pole pairs (P)	4

The FLC is considered a speed controller to initiate that the reference speed ( $W_{ref}$ ) is fixed to 400 rpm. The PI controller is regarded as a current controller to control the dq-axis stator current. The PI controller gain values like  $K_p$  and  $K_i$  are fixed to 10 and 1, respectively. The load torque ( $T_m$ ) is initially set to 0 Nm under no-load conditions, and the  $T_m$  values are varied from 2 to 10 Nm for different load conditions. The two PI controllers for the d and q current axis separately are considered in an inner current loop. The FLC is regarded as an outer speed loop. The 400 V dc-voltage is fed to the inverter module through the rectifier module. The SVPWM is used to provide the duty cycles or gate pulses to the inverter. The inverter is used to drive the PMSM to generate the controlled rotor speed.

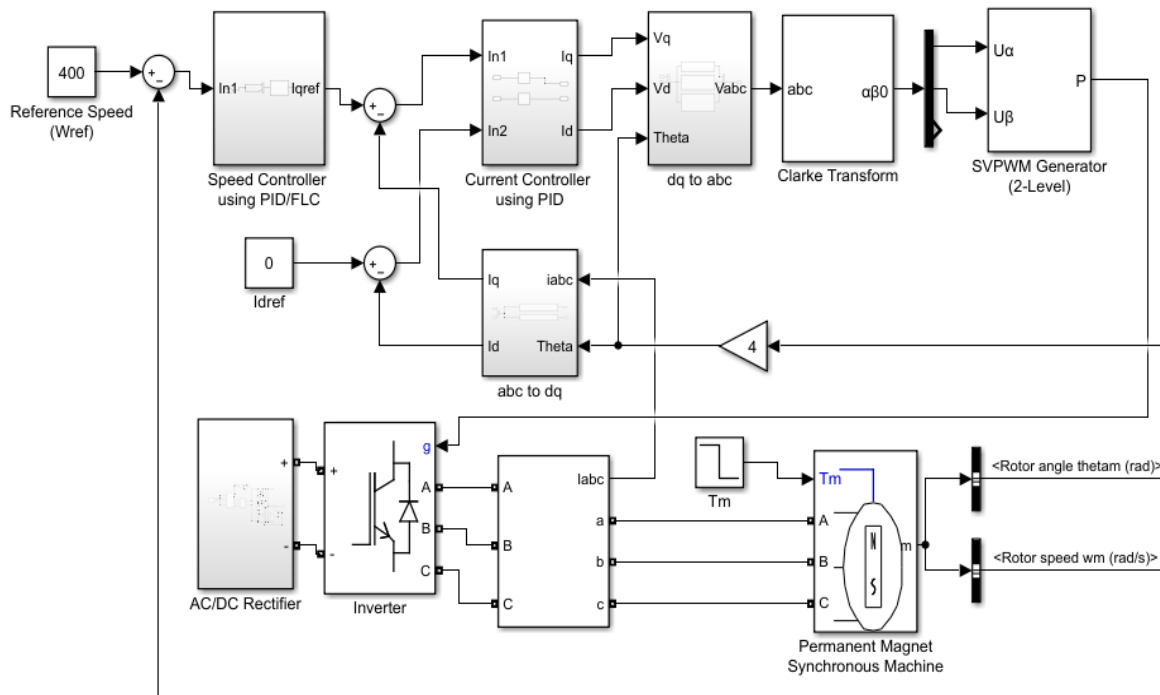


Figure 5. Modeling of PMSM using PID/FLC

The speed reference is fixed to 400 rpm, and torque load ( $T_m$ ) is set to 8 Nm at 0.05 sec. The dynamic response of the PID and FLC-based PMSM drive simulation results is represented in Figure 6. The speed response in Figure 6(a), speed error in Figure 6(b), and torque response in Figure 6(c) using PID controller and FLC are illustrated. The speed response settles at 0.09 sec, with an overshoot value of 0.0147% and the speed error is 0.023 rpm using PID controller for PMSM drive. The torque response settles at 0.09 sec to the steady state, starting at 8 Nm using the PID controller. The speed response settles at 0.055 sec, with an overshoot value of 0.015 % and the speed error is 0.0011 rpm using FLC for PMSM drive. The torque response settles at 0.055 sec to the steady state, starting at 8 Nm using FLC.

The three-phase stator current ( $I_{abc}$ ) of PID controller and FLC-based PMSM drive is represented in Figure 7. Initially, the three-phase current is very high and later reaches the steady-state value at 0.09 sec and 0.055 sec using the PID controller in Figure 7(a) and FLC in Figure 7(b), respectively for the PMSM drive system. The PID/FLC based PMSM drive performance analysis for the given torque load at 0.005 sec is tabulated in Table 3. The parameters like rising time, settling time, % overshoot, and steady-state error are considered for the comparative analysis between PID and FLC-based PMSM.

The performance comparison of PMSM dynamic responses with a torque load is represented in Figure 8. The torque load is varied from 0 to 10 Nm to analyze the response of the PMSM. The graphical representation of % overshoot time with torque load and speed error with torque load is shown in Figures 8(a) and 8(b). The FLC-based PMSM drive gives less overhead, improving 68.3% in settling time, 20.32% in overshoot time, and around 87.5% in steady-state error than PID-based PMSM under no-torque load conditions. Similarly, The FLC-based PMSM drive gives less overhead with an improvement of 37.62% settling time, 66.53% overshoot time, and around 87% steady-state error than PID-based PMSM under 10 Nm-torque load conditions.



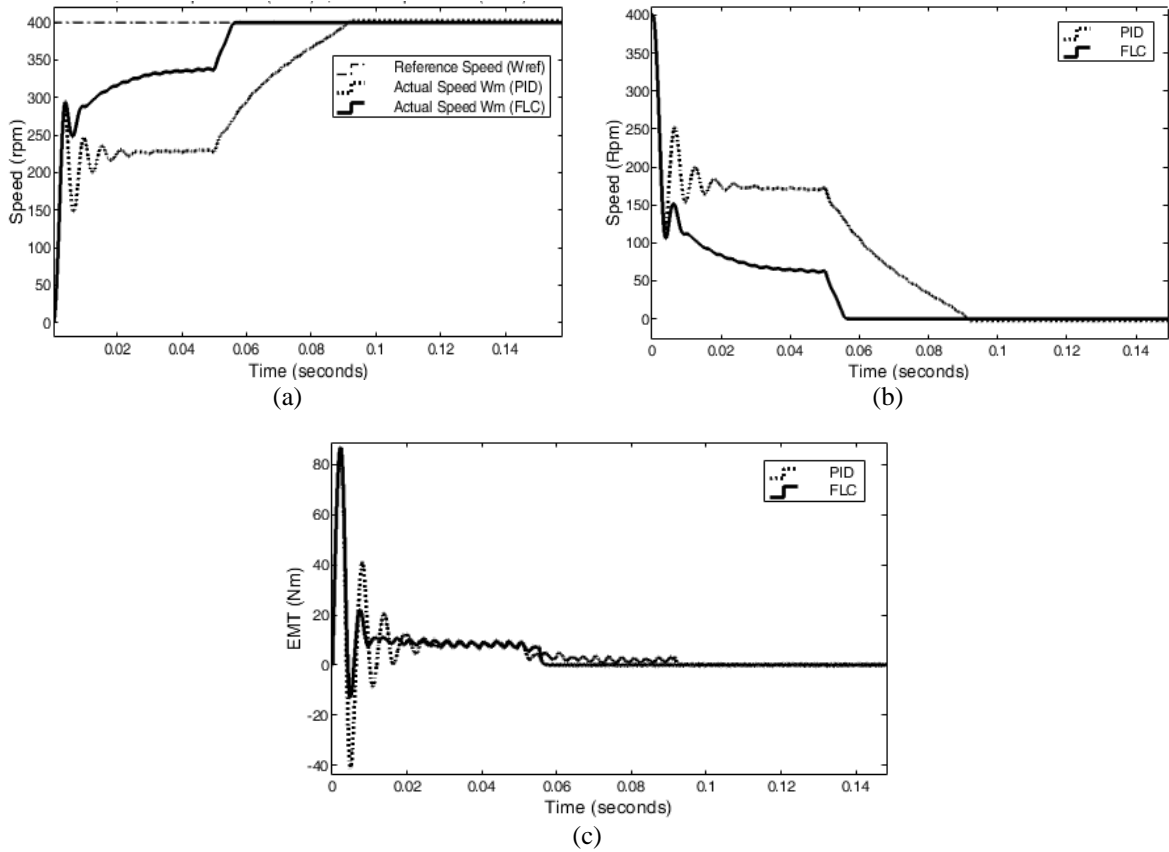


Figure 6. Dynamic response of PID/FLC based PMSM drive, (a) speed response, (b) speed error, and (c) torque response

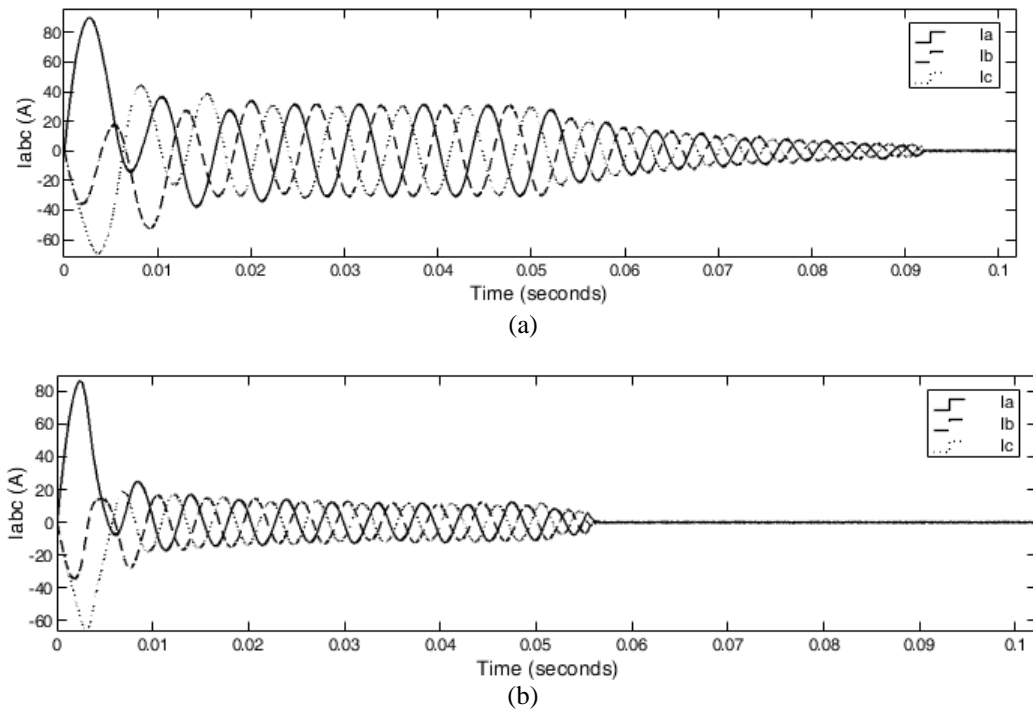


Figure 7. Three-phase stator current of PID and FLC based PMSM drive, (a) three-phase stator current ( $I_{abc}$ ) using PID, (b) three-phase stator current ( $I_{abc}$ ) using FLC

Table 3. Performance analysis of PID/FLC based PMSM for the given torque load

Torque Load	Rise Time (sec)		Settling time (sec)		% Overshoot Time		Steady State Error (%)	
	PID	FLC	PID	FLC	PID	FLC	PID	FLC
No Load	0.0321	0.01	0.0443	0.014	0.0064	0.0051	0.008	0.001
2 Nm	0.058	0.0124	0.0703	0.0175	0.0132	0.0142	0.012	0.001
4 Nm	0.0691	0.0163	0.0817	0.0241	0.0137	0.0084	0.017	0.001
6 Nm	0.0743	0.0263	0.0875	0.044	0.0141	0.0028	0.021	0.001
8 Nm	0.0769	0.0508	0.09	0.055	0.0147	0.015	0.023	0.0011
10 Nm	0.0794	0.0534	0.0925	0.0577	0.0245	0.0082	0.025	0.002

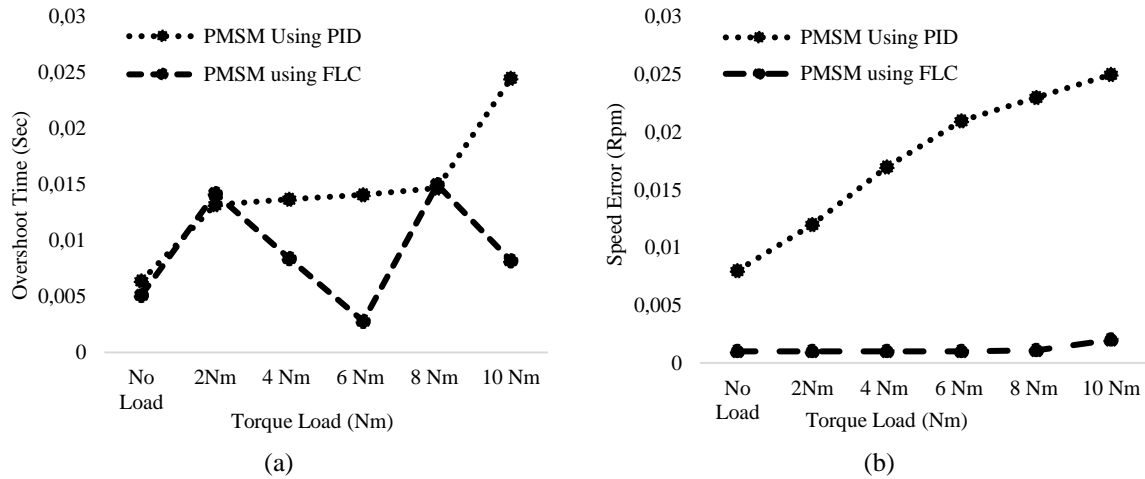


Figure 8. Performance comparison of PMSM dynamic responses with a torque load, (a) torque load (Nm) v/s overshoot time (%) (b) torque load (Nm) v/s speed error (Rpm)

The proposed FLC-based PMSM model is compared with similar FLC-based PMSM approaches [13], [17] and is represented in Table 4. The same torque load and dynamic response parameters are considered for the comparison. The proposed FLC-based PMSM drive provides a better dynamic response in settling time, overshoot time, and steady-state error than existing FLC-based PMSM approaches [13], [17]. Overall, the FLC-based PMSM drive gives rise time, overshoot time, settling time, and steady-state error parameter than the PID-based PMSM drive system. The triangular-based membership function is used in a fuzzy rule set to reduce the online operation calculation. The improved fuzzy rules with suitable display range improve the speed response faster, minimal overshoot time, and provide a better anti-interference ability. The FLC-based PMSM uses improved fuzzy rules to provide better control performance.

Table 4. Comparative analysis of FLC based PMSM with existing FLC based PMSM approaches

Parameters	Ref [13]	Proposed	Ref [17]	Proposed	Ref [17]	Proposed
	Load	10 Nm	0 Nm	2 Nm	2 Nm	2 Nm
Settling Time	0.05	0.057	0.5	0.014	0.62	0.0175
% Overshoot Time	0.026	0.0082	0.023	0.0051	0.024	0.0142
Steady state error	NA	0.002	0.0044	0.001	0.0026	0.001





### 5. CONCLUSION

In this manuscript, an efficient FLC-based PMSM drive is modeled to control the speed response of the motor. The FLC-based PMSM drive system mainly contains vector transformations, 2-level SVPWM, rectifier, inverter, and PMSM drive along with PI and fuzzy logic controllers. The improved fuzzy rules are used in each membership function of FLC to improve the dynamic response of the PMSM motor. The FLC controller is used as a speed controller compared with conventional PID controller based PMSM drive with performance improvements. The simulation results of speed response, speed error, torque response, and three-phase stator currents of PID and FLC-based PMSM drive are represented and discussed. The FLC-based PMSM drive system's speed response gives better settling time, less steady-state error, and minimal % overshoot time than the PID-based PMSM drive system and existing works.





## REFERENCES

- [1] G. Zhang, G. Wang, and D. Xu, "Saliency-based position sensorless control methods for PMSM drives-A review," *Chinese Journal of Electrical Engineering*, vol. 3, no. 2, pp. 14–23, Sep. 2017, doi: 10.23919/CJEE.2017.8048408.
- [2] Q. Wang, S. Wang, and C. Chen, "Review of sensorless control techniques for PMSM drives," *IEEJ Transactions on Electrical and Electronic Engineering*, vol. 14, no. 10, pp. 1543–1552, Oct. 2019, doi: 10.1002/tee.22974.
- [3] J. Yang, W.-H. Chen, S. Li, L. Guo, and Y. Yan, "Disturbance/uncertainty estimation and attenuation techniques in PMSM Drives-a survey," *IEEE Transactions on Industrial Electronics*, vol. 64, no. 4, pp. 3273–3285, Apr. 2017, doi: 10.1109/TIE.2016.2583412.
- [4] C. A. Lopez, W. R. Jensen, S. Hayslett, S. N. Foster, and E. G. Strangas, "A review of control methods for PMSM torque ripple reduction," in *2018 XIII International Conference on Electrical Machines (ICEM)*, Sep. 2018, pp. 521–526, doi: 10.1109/ICELMACH.2018.8507190.
- [5] Z. Wang, J. Yang, H. Ye, and W. Zhou, "A review of permanent magnet synchronous motor fault diagnosis," in *2014 IEEE Conference and Expo Transportation Electrification Asia-Pacific (ITEC Asia-Pacific)*, Aug. 2014, pp. 1–5, doi: 10.1109/ITEC-AP.2014.6940870.
- [6] P. Mattavelli, L. Tubiana, and M. Zigliotto, "Torque-ripple reduction in PM synchronous motor drives using repetitive current control," *IEEE Transactions on Power Electronics*, vol. 20, no. 6, pp. 1423–1431, Nov. 2005, doi: 10.1109/TPEL.2005.857559.
- [7] H. M. Hasanien, "Torque ripple minimization of permanent magnet synchronous motor using digital observer controller," *Energy Conversion and Management*, vol. 51, no. 1, pp. 98–104, Jan. 2010, doi: 10.1016/j.enconman.2009.08.027.
- [8] J.-W. Jung, Y.-S. Choi, V. Q. Leu, and H. H. Choi, "Fuzzy PI-type current controllers for permanent magnet synchronous motors," *IET Electric Power Applications*, vol. 5, no. 1, 2011, doi: 10.1049/iet-epa.2010.0036.
- [9] N. J. Patil, D. R. H. Chile, and D. L. M. Waghmare, "Fuzzy adaptive controllers for speed control of PMSM drive," *International Journal of Computer Applications*, vol. 1, no. 11, pp. 91–98, Feb. 2010, doi: 10.5120/233-387.
- [10] D. T. Govindaraj and R. V. Kumar, "AFLC based speed control of PMSM drive," *International Journal Of Advanced and Innovative Research*, pp. 433–439, 2012.
- [11] R. Na and X. Wang, "An improved vector-control system of PMSM based on fuzzy logic controller," in *2014 International Symposium on Computer, Consumer and Control*, Jun. 2014, pp. 326–331, doi: 10.1109/IS3C.2014.92.
- [12] A. Iqbal, H. Abu-Rub, and H. Nounou, "Adaptive fuzzy logic-controlled surface mount permanent magnet synchronous motor drive," *Systems Science and Control Engineering*, vol. 2, no. 1, pp. 465–475, Dec. 2014, doi: 10.1080/21642583.2014.915203.
- [13] S. P. Singh, A. K. Gautam, J. Dubey, J. P. Pandey, and R. P. Payasi, "Performance comparison of PMSM drive using PI and fuzzy logic based controllers," in *2016 IEEE Uttar Pradesh Section International Conference on Electrical, Computer and Electronics Engineering (UPCON)*, 2016, pp. 563–569, doi: 10.1109/UPCON.2016.7894716.
- [14] M. Umabharathi and S. Vijayabaskar, "Speed control of permanent magnet synchronous motor using evolutionary fuzzy PID controller," *International Journal of Electrical and Information Engineering*, vol. 9, no. 12, pp. 1485–1491, Dec. 2016.
- [15] E. Lazarescu, F. M. Frigura-Iliasa, P. Andea, and M. Frigura-Iliasa, "Speed control for a permanent magnet synchronous motor based on fuzzy logic with reduced perturbations on the supply network," in *2016 Electric Power Quality and Supply Reliability (PQ)*, Aug. 2016, pp. 207–212, doi: 10.1109/PQ.2016.7724114.
- [16] J. Liu, C. Gong, Z. Han, and E. Zhang, "An improved adaptive fuzzy PID controller for PMSM and a novel stability analysis method," in *2017 IEEE 3rd International Future Energy Electronics Conference and ECCE Asia (IFEEC 2017-ECCE Asia)*, Jun. 2017, pp. 2161–2164, doi: 10.1109/IFEEC.2017.7992386.
- [17] A. A. Abd Samat, M. Fazli, N. Salim, A. M. S. Omar, and M. K. Osman, "Speed control design of permanent magnet synchronous motor using Takagi-Sugeno fuzzy logic control," *Journal of Electrical Systems*, vol. 13, no. 4, pp. 689–695, 2017.
- [18] G. Rathod, A. G. Thosar, V. P. Dhote, and R. Zalke, "PM synchronous motor drive for electric vehicles by using an adaptive controller," in *2018 International Conference on Emerging Trends and Innovations In Engineering And Technological Research (ICETIETR)*, Jul. 2018, pp. 1–5, doi: 10.1109/ICETIETR.2018.8529029.
- [19] K. S. Gaeid, M. A. Asker, N. N. Tawfeeq, and S. R. Mahdi, "Computer simulation of PMSM motor with five phase inverter control using signal processing techniques," *International Journal of Electrical and Computer Engineering (IJECE)*, vol. 8, no. 5, pp. 3697–3710, Oct. 2018, doi: 10.11591/ijece.v8i5.pp3697-3710.
- [20] P. Lu, M. Gu, Y. Yang, H. Zhao, and Y. Wu, "Research on adaptive control of PMSM based on fuzzy PID," in *2019 IEEE 3rd Advanced Information Management, Communicates, Electronic and Automation Control Conference (IMCEC)*, Oct. 2019, pp. 1565–1569, doi: 10.1109/IMCEC46724.2019.8983879.
- [21] T. Hu and X. Zhang, "Simulation of PMSM vector control system based on fuzzy PI controller," in *2019 IEEE International Conference on Power, Intelligent Computing and Systems (ICPICS)*, Jul. 2019, pp. 111–114, doi: 10.1109/ICPICS47731.2019.8942439.
- [22] K. Kakouche, W. Guendouz, T. Rekioua, S. Mezani, and T. Lubin, "Application of fuzzy controller to minimize torque and flux ripples of PMSM," in *2019 International Conference on Advanced Electrical Engineering (ICAEE)*, Nov. 2019, pp. 1–6, doi: 10.1109/ICAEE47123.2019.9015066.
- [23] Y. Xue, H. Yu, and X. Liu, "Improved fuzzy backstepping position tracking control for manipulator driven by PMSM," in *2018 Chinese Automation Congress (CAC)*, Nov. 2018, pp. 3561–3565, doi: 10.1109/CAC.2018.8623601.
- [24] A. Balashanmugham and M. Maheswaran, "Permanent-magnet synchronous machine drives," in *Applied Electromechanical Devices and Machines for Electric Mobility Solutions*, IntechOpen, 2020, doi: 10.5772/intechopen.88597.
- [25] K. Urbanski and D. Janiszewski, "Sensorless control of the permanent magnet synchronous motor," *Sensors*, vol. 19, no. 16, Aug. 2019, doi: 10.3390/s19163546.
- [26] N. H. Hadi and I. K. Ibraheem, "Speed control of an SPMSM using a tracking differentiator-PID controller scheme with a genetic algorithm," *International Journal of Electrical and Computer Engineering (IJECE)*, vol. 11, no. 2, pp. 1728–1741, Apr. 2021, doi: 10.11591/ijece.v11i2.pp1728-1741.
- [27] K. Viji, A. Kumar, and R. Nagaraj, "Improved delta operator based discrete sliding mode fuzzy controller for buck converter," *Indian Journal of Science and Technology*, vol. 10, no. 25, pp. 1–11, Feb. 2017, doi: 10.17485/ijst/2017/v10i25/116507.
- [28] K. Viji, K. Chitra, T. Someswari, M. Raichel Ruby, and P. Sandhya, "Solar powered DC motor speed control by MPPT and discrete controller," in *2021 Third International Conference on Intelligent Communication Technologies and Virtual Mobile Networks (ICICV)*, Feb. 2021, pp. 651–655, doi: 10.1109/ICICV50876.2021.9388556.

**BIOGRAPHIES OF AUTHORS**

**Parvathy Thampi Mooloor Sahridayan**     currently working as an Assistant Professor in CMRIT College of Engineering, Bangalore, India. She has completed B. Tech in Electrical and Electronics from Govt. College of Engineering, Thiruvananthapuram, Kerala, India, and M. Tech from Oxford College of Engineering, Bangalore, India. She is pursuing her Ph.D. at Visvesvaraya Technological University (VTU), Belagavi, India. She is a competent professional with 13+ years of rich teaching experience in delivering Electrical and Electronics Engineering lectures. She can be contacted at email: parvathy.t@cmrit.ac.in.



**Raghavendra Gopal**     currently working as an Associate Professor, EEE in Saphagiri College of Engineering, Bengaluru, India. He has completed Ph.D. from JAIN University in the specialization of Power Systems in 2018. He has 17+ years of rich teaching experience. He has published 10+ national and international journals and Conference Papers. He can be contacted at email: raghavendrag@sapthagiri.edu.in.